

# Contouring Control of a Parallel Mechanism Based on Equivalent Errors

Shyh-Leh Chen

Department of Mechanical Engineering  
National Chung-Cheng University  
Chia-Yi 621, TAIWAN

Email: imeslc@ccu.edu.tw

Yuan-Cheng Tsai

Department of Mechanical Engineering  
National Chung-Cheng University  
Chia-Yi 621, TAIWAN

**Abstract**— This study is concerned with the contouring control of a parallel mechanism, which is a constrained multi-axis motion system. The method of equivalent errors, previously proposed for unconstrained systems, is applied to design a contouring controller for such systems. It is found that the definition of equivalent errors is not affected by constraints. Hence, the design procedure of contouring controller is exactly the same as that for the unconstrained system. Due to the constraints, however, the state variables in the control law are not fully independent. Some of the states, which are not available from measurement, are actually function of the other available states. In general, it is impossible to directly solve the constraint equation that may contain transcendental functions. Therefore, a linear approximation is used to estimate the unavailable states. Numerical simulations are carried out for the contouring of several paths, including circular and elliptic paths. The results indeed confirm the validity of the proposed method.

## I. INTRODUCTION

SINCE the development of the well known Stewart platform [1], there have been considerable developments of parallel mechanisms as they can be found in industrial robots, simulators, micromanipulators and parallel machine tools, see, e.g., [2-7]. Parallel manipulators have many advantages over serial manipulators, such as less error accumulation and supporting higher load/weight [2]. The main disadvantage of parallel mechanisms is its complicated kinematics and system dynamics. As a result, the contouring control of such system is a nontrivial task. There have been several methods proposed for this purpose [8-13]. Among them, the method of equivalent errors [13] is especially suitable for parallel motion systems. For a motion system with  $n$  axes, the equivalent errors include  $n-1$  equivalent errors and 1 tangential error, which are defined utilizing the algebraic equations determining the desired path. Under proper assumptions, reducing the equivalent errors is equivalent to reducing the actual contour error. By transforming the system dynamics into the coordinates of equivalent errors, the contouring control problem will become the stabilization problem. Then stabilization control methods can be employed to yield the contouring controller.

The method of equivalent errors possesses several

advantages over conventional contouring control methods. For details, please refer to [13]. In particular, it is suitable for complicated nonlinear systems following complicated paths with high speed. Under such extreme situation, large contour errors are in general inevitable for conventional methods. The objective of this paper is to design a contouring controller for a complicated parallel mechanism by the method of equivalent errors.

## II. SYSTEM DESCRIPTION

Fig. 1 shows the machine tool consisting of the parallel mechanism considered in this study. The detailed schematic of the parallel mechanism is shown in Fig. 2. It has been analyzed in several studies [4-7]. It consists of one fixed base platform and one moving platform connected by 3 links. The base platform is a triangle with vertices denoted by  $A_1, A_2, A_3$ . The moving platform is also a triangle with vertices denoted by  $T_1, T_2, T_3$ . There are 3 vertical beams attached to base platform at  $A_1, A_2, A_3$ . Three sliders denoted by  $B_1, B_2, B_3$  can slide on the vertical beams. Servomotors with ball-screws are used to actuate the sliding motion. Three links of constant length  $L$  connect the sliders to the moving platform. As a result, the sliding motion on the vertical beams will cause the motion of the moving platform. The motion system has three types of joints. The first type is the prismatic joint connecting the base platform and the slider. The second type is the revolute joint connecting the slider and the link. The third type is the spherical joint connecting the moving platform and the link. Therefore, the system is referred to as three-PRS (Prismatic-Revolute-Spherical) parallel manipulator. Please refer to [4-7] for detailed description of the system.

## III. DYNAMIC EQUATIONS

The three-PRS system possesses 3 degrees of freedom with complicated forward and backward kinematics. For brevity, only necessary results are presented here. Detailed derivation of the dynamic equations of the three-PRS parallel mechanism can be found in [7].

It is assumed that no friction exists on the joints and the components of the mechanism are rigid. Although the system is 3-DOF, it is more convenient to represent its dynamics by 6 generalized coordinates, i.e.,

$$x = [S_1 \ S_2 \ S_3 \ \theta_1 \ \theta_2 \ \theta_3]^T$$

where  $x_a = [S_1 \ S_2 \ S_3]^T$  are the stretch lengths of the ball screw (i.e.,  $S_i = \text{length of } \overline{A_i B_i}$ ), and  $x_b = [\theta_1 \ \theta_2 \ \theta_3]^T$  are the angles between the links  $\overline{B_i T_i}$  and the horizontal plane, as shown in Fig. 2. The 6 generalized coordinates are not independent. They must satisfy 3 geometric constraints represented by

$$\phi(x) = [\phi_1(x) \ \phi_2(x) \ \phi_3(x)]^T = 0 \quad (1)$$

The constraints are obtained by the fact that the side lengths of the triangle of the moving platform are constant. The functions  $\phi_i(x)$  are complicated and their expressions are omitted for simplicity. For the constraint, it is assumed that  $\frac{\partial \phi}{\partial x_b}$  is nonsingular. By implicit function theorem [14], this assumption implies that there exists a unique solution at least locally of the form

$$x_b = \psi(x_a) \quad (2)$$

for equation (1). If equation (2) can be obtained, the system dynamics can be well represented by  $x_a$  only. Unfortunately, equation (2) is in general unavailable since equation (1) in general involves transcendental algebraic equations. The dynamic equations can be derived by the Lagrangian approach and are given by

$$\begin{aligned} [r \tan \rho M(x) + J] \ddot{x} \\ + r \tan \rho [C(x, \dot{x}) \dot{x} + K(x) + \phi_x^T \lambda] = \tau_a \end{aligned} \quad (3)$$

with the  $6 \times 6$  matrix  $J$  given by

$$J = \begin{bmatrix} J_D & 0_{3 \times 3} \\ 0_{3 \times 3} & 0_{3 \times 3} \end{bmatrix}$$

where  $\lambda$  is the Lagrange's multiplier due to the constraint;  $r$  and  $\rho$  are the radius and the lead angle of the ball screw;  $M(x)$  is a nonsingular inertial matrix,  $C(x, \dot{x})$  represents the gyroscopic and damping matrix,  $K(x)$  contains the gravitational forces;  $\phi_x = \partial \phi / \partial x$ ;  $\tau_a = [\tau_1 \ \tau_2 \ \tau_3 \ 0 \ 0 \ 0]^T$ ,  $\tau_i$  are the output torques of the three actuating motors;  $J_D = \text{diag}(J', J', J')$   $J' = (J_1 + J_2) * 2\pi / \sigma$ , where  $J_1$  and  $J_2$  are the rotational inertias of the ball screws and that of

actuating motor respectively, and  $\sigma$  is the pitch of the ball screws. Again, the expressions of  $M(x)$ ,  $C(x, \dot{x})$ , and  $K(x)$  are complicated and are omitted.

Let  $\alpha = r \tan \rho$ ,  $M_1(x) = \alpha M(x) + J$ , and  $q_1(x, \dot{x}) = \alpha [C(x, \dot{x}) \dot{x} + K(x)]$ . Then, equation (3) can be rewritten as

$$M_1(x) \ddot{x} + \alpha \phi_x^T(x) \lambda + q_1(x, \dot{x}) = \tau_a \quad (4)$$

It can be shown that the inertial matrix  $M_1(x)$  is positive definite. Hence, from (4), one can get

$$\ddot{x} = -\alpha M_1^{-1} \phi_x^T \lambda - M_1^{-1} q_1 + M_1^{-1} \tau_a \quad (5)$$

where the arguments  $x$  and  $\dot{x}$  in  $M_1$ ,  $q_1$ ,  $\phi$  are omitted for simplicity. On the other hand, from the constraint (1), one can get

$$\ddot{\phi} = \phi_x \ddot{x} + (\phi_x \dot{x})_x \dot{x} = 0 \quad (6)$$

Inserting (5) into (6) gives

$$\alpha M_2(x) \lambda = q_2(x, \dot{x}) + \phi_x M_1^{-1} \tau_a \quad (7)$$

where  $M_2(x) = \phi_x M_1^{-1} \phi_x^T$  is a positive matrix since  $\phi_x$  is of full rank, and  $q_2(x, \dot{x}) = -\phi_x M_1^{-1} q_1 + (\phi_x \dot{x})_x \dot{x}$ . Hence, equation (7) yields

$$\alpha \lambda = M_2^{-1} q_2 + M_2^{-1} \phi_x M_1^{-1} \tau_a \quad (8)$$

Thus, the Lagrange's multiplier  $\lambda$  can be eliminated by plugging (8) into (5), resulting in

$$\ddot{x} = f(x, \dot{x}) + G_1(x) \tau_a \quad (9)$$

where

$$f(x, \dot{x}) = -M_1^{-1} \phi_x^T M_2^{-1} q_2 - M_1^{-1} q_1 \quad (10)$$

$$G_1(x) = M_1^{-1} - M_1^{-1} \phi_x^T M_2^{-1} \phi_x M_1^{-1} \quad (11)$$

Let  $G(x)$  be the  $3 \times 3$  matrix formed by the first 3 columns of  $G_1(x)$ . Equation (9) can be written as

$$\ddot{x} = f(x, \dot{x}) + G(x) \tau \quad (12)$$

where  $\tau = [\tau_1 \ \tau_2 \ \tau_3]^T$ .

Next, it is to show that  $G(x)$  is nonsingular. To this aim, the following lemma is needed. Let  $N(A)$  denote the null space of a matrix  $A$ , and  $Col(A)$  denotes its column space.

*Lemma:*  $N(G_1) = \text{Col}(\phi_x^T)$

*proof:* First, it is easy to see that

$$G_1 \phi_x^T = M_1^{-1} \phi_x^T - M_1^{-1} \phi_x^T = 0$$

implying that

$$\text{Col}(\phi_x^T) \subset N(G_1) \quad (13)$$

On the other hand,  $\forall v \in N(G_1)$  and  $v \neq 0$ , we have

$$G_1 v = 0 \Rightarrow M_1^{-1} v = M_1^{-1} \phi_x^T M_2^{-1} \phi_x M_1^{-1} v$$

which is equivalent to

$$v = \phi_x^T u \quad (14)$$

where  $u = M_2^{-1} \phi_x M_1^{-1} v$ . Clearly,  $u \neq 0$  (otherwise  $v = 0$ ).

Equation (14) implies that  $v \in \text{Col}(\phi_x^T)$ . Hence

$$N(G_1) \subset \text{Col}(\phi_x^T) \quad (15)$$

Equations (13) and (15) imply that

$$N(G_1) = \text{Col}(\phi_x^T)$$

which completes the proof of the lemma.

Now, consider a vector  $\beta \in \mathfrak{R}^6$  defined by

$$\beta = [\beta_1 \quad \beta_2 \quad \beta_3 \quad 0 \quad 0 \quad 0]^T$$

where  $\beta_i$  are not all zero, Since  $\frac{\partial \phi}{\partial x_b}$  is nonsingular, it is

clear that  $\beta \notin \text{Col}(\phi_x^T)$ , and hence  $\beta \notin N(G_1)$ . In other words,

$$G_1 \beta \neq 0 \quad (16)$$

implying that any linear combination of the first 3 columns of  $G_1$  is not zero. Hence, the first 3 columns of  $G_1$  are linearly independent and thus  $G(x)$  is of full rank.

#### IV. CONTROLLER DESIGN

In this section, we will use the method of equivalent errors to design a contouring controller for the three-PRS parallel manipulator. Since the system is 3-DOF, the desired path can be described by two algebraic equations in the generalized coordinates, i.e.,  $p_1(x_d) = 0$  and  $p_2(x_d) = 0$ . Here,  $x_d(t)$  represents the position command. Thus, the

contour errors  $\varepsilon \in R^2$  and the tangential error  $e \in R$  are defined by

$$\varepsilon_1 = p_1(x), \quad \varepsilon_2 = p_2(x), \quad \text{and} \quad e = \dot{x}_d^T (x - x_d)$$

Then, the error dynamics can be obtained in the form

$$\begin{bmatrix} \ddot{\varepsilon}_1 \\ \ddot{\varepsilon}_2 \\ \ddot{e} \end{bmatrix} = \Omega(x, \dot{x}, t) + \Gamma(x, \dot{x}, t) \tau \quad (17)$$

where  $\Gamma(x, \dot{x}, t)$  is a nonsingular matrix since  $G(x)$  is of full rank. Again, the detailed expressions of  $\Omega$  and  $\Gamma$  are omitted. With the error dynamics, one can now design a stabilizing controller that will be a contouring controller for the motion system. Since  $\Gamma(x, \dot{x}, t)$  is nonsingular, the controller can be designed by feedback linearizing the error dynamics first, and then followed by a robust controller, such as sliding mode controller [15].

The contouring controller obtained above will be a function of the generalized displacements  $x$  and velocities  $\dot{x}$ . However, only  $x_a$  is available from measurement. The other, i.e.,  $x_b$ , can be obtained from the constraint equation. To this aim, the constraint equation is expanded in Taylor series with respect to the desired command  $x = x_d = [x_{da} \quad x_{db}]^T$ , yielding

$$\phi(x_d) + \frac{\partial \phi}{\partial x_a} \Big|_{x_d} (x_a - x_{da}) + \frac{\partial \phi}{\partial x_b} \Big|_{x_d} (x_b - x_{db}) + O(2) = 0 \quad (18)$$

where  $O(2)$  denotes higher order terms. Since  $\|x - x_d\|$  is in general small, equation (18) can be approximated by

$$\frac{\partial \phi}{\partial x_a} \Big|_{x_d} (x_a - x_{da}) + \frac{\partial \phi}{\partial x_b} \Big|_{x_d} (x_b - x_{db}) \approx 0 \quad (19)$$

Hence,  $x_b$  can be estimated by

$$\hat{x}_b = x_{db} - A_2^{-1} A_1 (x_a - x_{da}) \quad (20)$$

where  $A_1 = \frac{\partial \phi}{\partial x_a} \Big|_{x_d}$  and recall that  $A_2 = \frac{\partial \phi}{\partial x_b} \Big|_{x_d}$  is of full rank.

On the other hand, differentiating the constraint  $\phi(x) = 0$  gives

$$\frac{\partial \phi}{\partial x_a} \dot{x}_a + \frac{\partial \phi}{\partial x_b} \dot{x}_b = 0 \Rightarrow \hat{\dot{x}}_b = - \left[ \frac{\partial \phi}{\partial x_b} \right]^{-1} \left[ \frac{\partial \phi}{\partial x_a} \right] \dot{x}_a \quad (21)$$

#### V. NUMERICAL RESULTS AND DISCUSSIONS

The above analysis will be verified through numerical simulations in this section. It is hoped that the cutter end

point will follow a given desired path. The cutter is a vertical link connected to the center of the moving plate, as shown in Fig. Let  $(X_C, Y_C, Z_C)$  be the position of the cutter end point, which is a function of the generalized coordinates  $x$ . Again, this complicated function is omitted for brevity.

Two desired paths will be followed:

- (i) a circular path with radius  $r_d = 50\text{mm}$  and angular velocity  $\omega_d = 6\text{rad/s}$ , i.e.,  $X_{Cd} = 0.05\cos(\omega_d t)$ ,  $Y_{Cd} = 0.05\sin(\omega_d t) + 0.1745$ , and  $Z_{Cd} = -1.4$ .
- (ii) an elliptic path with the lengths of two axes being  $a = 50\text{mm}$  and  $b = 30\text{mm}$ , and  $\omega_d = 6\text{rad/s}$ , i.e.,  $X_{Cd} = 0.05\cos(\omega_d t)$ ,  $Y_{Cd} = 0.03\sin(\omega_d t) + 0.1745$ , and  $Z_{Cd} = -1.4$ .

For the circular path, the equivalent contour errors  $\varepsilon_1, \varepsilon_2$  and the tangential error  $e$  are given by

$$\begin{aligned}\varepsilon_1 &= X_C^2 + (Y_C - 0.1745)^2 - 0.05^2 \\ \varepsilon_2 &= Z_C - (-1.4) \\ e &= \dot{X}_{Cd}(X_C - X_{Cd}) + \dot{Y}_{Cd}(Y_C - Y_{Cd}) + \dot{Z}_{Cd}(Z_C - Z_{Cd})\end{aligned}$$

For the elliptic path, the equivalent contour errors  $\varepsilon_1, \varepsilon_2$  and the tangential error  $e$  are given by

$$\begin{aligned}\varepsilon_1 &= \left(\frac{X_C}{0.05}\right)^2 + \left(\frac{Y_C - 0.1745}{0.03}\right)^2 - 1 \\ \varepsilon_2 &= Z_C - (-1.4) \\ e &= \dot{X}_{Cd}(X_C - X_{Cd}) + \dot{Y}_{Cd}(Y_C - Y_{Cd}) + \dot{Z}_{Cd}(Z_C - Z_{Cd})\end{aligned}$$

With the equivalent errors, we can now follow the procedure outlined in the previous section to design a contouring controller. This will be done by feedback linearization followed by an integral sliding mode control [6]. In other words, the control law for the input torques is

$$\tau = \begin{bmatrix} \tau_1 \\ \tau_2 \\ \tau_3 \end{bmatrix} = \Gamma^{-1} \begin{bmatrix} \Omega_1 - b\dot{\varepsilon}_1 - c\varepsilon_1 - \frac{\mu_1 + \mu_2}{1-k} \text{sat}\left(\frac{\sigma_1}{\delta}\right) \\ \Omega_2 - b\dot{\varepsilon}_2 - c\varepsilon_2 - \frac{\mu_1 + \mu_2}{1-k} \text{sat}\left(\frac{\sigma_2}{\delta}\right) \\ \Omega_3 - b\dot{e} - ce - \frac{\mu_1 + \mu_2}{1-k} \text{sat}\left(\frac{\sigma_3}{\delta}\right) \end{bmatrix}$$

where

$$\begin{aligned}\sigma_1 &= \dot{\varepsilon}_1 + b\varepsilon_1 + c\varepsilon_1 = 0, & \dot{z}_1 &= \varepsilon_1 \\ \sigma_2 &= \dot{\varepsilon}_2 + b\varepsilon_2 + c\varepsilon_2 = 0, & \dot{z}_2 &= \varepsilon_2 \\ \sigma_3 &= \dot{e} + be + ce = 0, & \dot{z}_3 &= e\end{aligned}$$

are the integral sliding manifolds.

For the following simulations, the control parameters

are chosen as

$$b = 40, c = 400, \mu_1 = 8, \mu_2 = 5, k = 0.5 \text{ and } \delta = 0.1$$

For both the circular and elliptic paths, three cases of parameter variations are considered: (i) no uncertainty; (ii) 25% of variation in system parameters; (iii) 50% of variation in system parameters. Fig. 3 shows the simulation results for the actual contour errors. Without uncertainty, the contour error reaches the steady state in about 0.5sec, with steady state contour error less than  $0.1\mu\text{m}$ . With uncertainty, the steady state contour error will be oscillating. The magnitude is about  $1\mu\text{m}$  for case (ii) and  $2\mu\text{m}$  for case (iii). The average contour error (ACE) defined by

$$\bar{\varepsilon} = \frac{1}{N} \sum_{i=1}^N |\varepsilon_c(i)|$$

where  $\varepsilon_c$  is the actual contour error, is  $0.773\mu\text{m}$  for case (i),  $5.532\mu\text{m}$  for case (ii), and  $9.429\mu\text{m}$  for case (iii). Although the larger uncertainty will cause larger contour errors, the ISMC controller can still keep them in a reasonable range. Thus, one can conclude that the ISMC contouring controller works for this complicated multi-axis parallel motion system even with large uncertainty. Similar conclusions also apply to the contouring control of the elliptic path, whose simulation results are presented in Fig. 4.

## VI. CONCLUSIONS

The method of equivalent errors has been applied to design a contouring controller for a parallel motion system. The equivalent errors allow one to transform the contouring problem into the error stabilization problem. Then, either feedback stabilization with integral sliding mode control can be used to design the controller. Because of the constraints, the states in the control law are not completely independent. The unavailable states can be estimated using linear approximation from the constraint equation. Simulation results verify the proposed method.

## VII. REFERENCES

- [1] D. Stewart, "A platform with Six Degrees of Freedom," *Proceedings of IME*, Vol. 180, No. 5, pp. 371-386, 1965.
- [2] Xin-Jun Liu, Jinsong Wang, Feng Gao, and Li-Ping Wang, "On the Analysis of a New Spatial Three-Degree-of-Freedom Parallel Manipulator," *IEEE Transactions on Robotics and Automation*, Vol. 17, No. 6, Dec. 2001.
- [3] Goldsmith, P.B., "Design and kinematics of a three-legged parallel manipulator," *IEEE Transactions on Robotics and Automation*, Vol. 19, No. 4, pp. 726-731, Aug. 2003.
- [4] Tsai, M. S., T. N. Shiau, Y. J. Tsai, and T. H. Chang, "Direct Kinematic Analysis of a 3-PRS Parallel Mechanism," *Mechanism and Machine Theory*, Vol. 38, No. 1, 2003, pp. 71-83.
- [5] K.C. Fan, H. Wang, J.W. Zhao, and T.H. Chang, "Sensitivity analysis of the 3-PRS parallel kinematic platform of a serial-parallel

machine tool,” *International Journal of Machine Tools and Manufacture*, Vol. 43, 2003, pp. 1561–1569.

- [6] H. Wang and K.-C. Fan, “Identification of strut and assembly errors of a 3-PRS serial-parallel machine tool,” *International Journal of Machine Tools and Manufacture*, Vol. 44, 2004, pp. 1171–1178.
- [7] T. N. Shiau, Y. J. Tsai, and M. S. Tsai, “Nonlinear dynamic analysis of a parallel mechanism with consideration of joint effects,” *Mechanism and Machine Theory*, 2007 (accepted).
- [8] K. Srinivasan and T.C. Tsao, “Machine tool feed drives and their control—a survey of the state of the art,” *ASME Journal of Manufacturing Science and Engineering*, Vol. 119, pp. 743-748, 1997.
- [9] G. T.-C. Chiu, “Contour Tracking of Machine Tool Feed Drive Systems,” *Proceedings of the American Control Conference*, Philadelphia, Pennsylvania, USA, pp. 3833-3837, June 1998.
- [10] G. T.-C. Chiu and M. Tomizuka, “Coordinated Position Control of Multi-Axis Mechanical Systems,” *ASME Journal of Dynamic Systems, Measurement and Control*, Vol. 120, pp. 389-393, Sep 1998.
- [11] S.-S. Yeh and P.-L. Hsu, “Analysis and Design of the Integrated Controller for Precise Motion Systems,” *IEEE Transactions on Control System Technology*, Vol. 7, No. 6, pp. 706-717, November 1999.
- [12] Shyh-Leh Chen, Hung-Liang Liu, and Sing Ching Ting, “Contouring Control of Biaxial Systems Based on Polar Coordinates,” *IEEE/ASME Transactions on Mechatronics*, Vol. 7, No. 3, 2002, pp.329-345.
- [13] Shyh-Leh Chen and Kai-Chiang Wu, “Contouring Control of Smooth Paths for Multi-axis Systems Based on Equivalent Errors,” *IEEE Transactions on Control Systems Technology*, Vol. 15, No. 6, 2007.
- [14] T. M. Apostol, *Mathematical Analysis*, 2nd ed., Menlo Park, California: Addison-Wesley, 1974.
- [15] H. K. Khalil, *Nonlinear Systems*, 2nd ed., Prentice Hall, New Jersey, 1996.

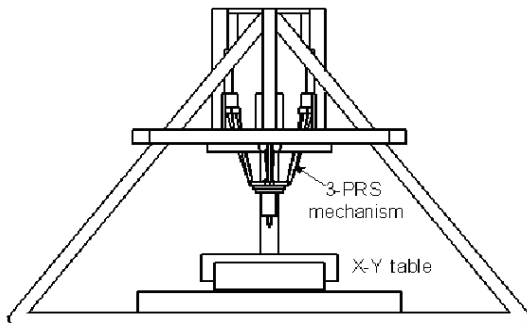


Fig. 1 The 3-PRS mechanism in a machine tool

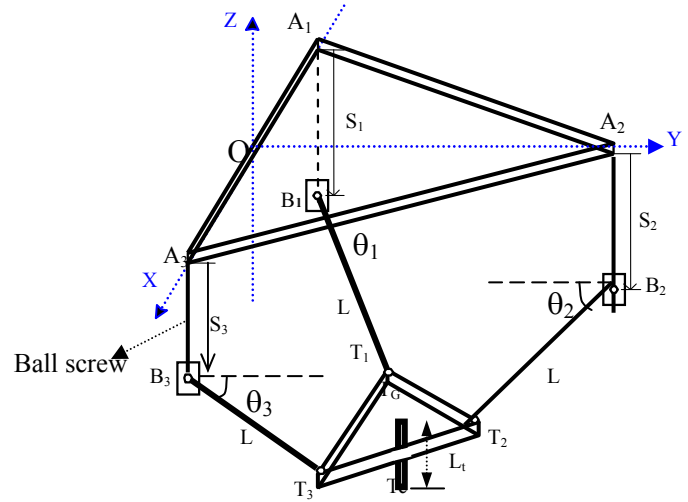


Fig. 2 The schematics of the 3-PRS parallel mechanism

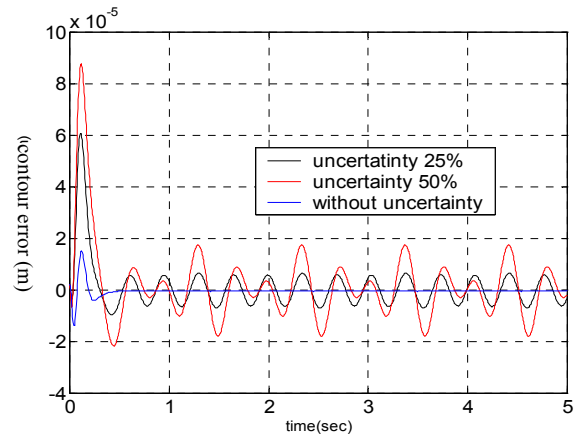


Fig. 3 Contour errors of circular path

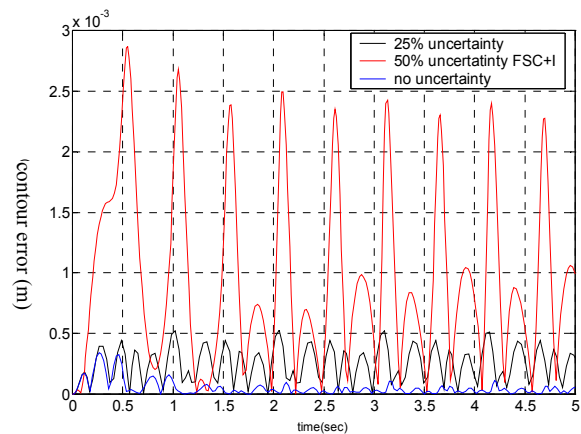


Fig. 4 Contour errors of elliptic path